



Degradation of a polymer exchange membrane fuel cell stack with Nafion[®] membranes of different thicknesses: Part I. In situ diagnosis

Xiao-Zi Yuan^a, Shengsheng Zhang^a, Haijiang Wang^{a,*}, Jinfeng Wu^a, Jian Colin Sun^a, Renate Hiesgen^b, K. Andreas Friedrich^c, Mathias Schulze^c, Andrea Haug^c

^a Institute for Fuel Cell Innovation, National Research Council Canada, Vancouver, BC, Canada V6T 1W5

^b University of Applied Sciences Esslingen, Department of Basic Science, Kanalstrasse 33, 73728 Esslingen, Germany

^c Institute of Technical Thermodynamics, German Aerospace Center, Pfaffenwaldring 38-40, 70569 Stuttgart, Germany

ARTICLE INFO

Article history:

Received 4 May 2010

Received in revised form 8 June 2010

Accepted 9 June 2010

Available online 16 June 2010

Keywords:

Proton exchange membrane fuel cell

Stack

In situ

Durability

Idle conditions

Degradation

ABSTRACT

The durability of polymer exchange membrane (PEM) fuel cells, under a wide range of operational conditions, has been attracting intensive attention, as durability is one of the largest barriers for commercialization of this promising technology. In the present work, membrane electrode assembly (MEA) degradation of a four-cell stack with Nafion membranes of different thicknesses, including N117, N115, NR212, and NR211, was carried out for 1000 h under idle conditions. By means of several on-line electrochemical measurements, the performance of the individual cells was analyzed at different times during the degradation process. The results indicate that the cells with thinner membranes have a lower open circuit voltage (OCV) due to the higher fuel crossover. Before degradation, the thickness of the membranes correlates with performance of the cell. However, with the advancement of degradation, the performance of cells with thinner membranes degraded much faster than those with thicker membranes, especially after 800 h of operation. The fast performance degradation for thinner membranes is evident by a dramatic increase in hydrogen crossover indicating membrane thinning or pinhole formation.

Crown Copyright © 2010 Published by Elsevier B.V. All rights reserved.

1. Introduction

The durability of proton exchange membrane (PEM) fuel cells is one of the biggest challenges and barriers for commercializing this promising technology. As a result, numerous research activities have investigated the failure modes of degradation in order to reduce the wide gap that exists between the ideal and the state-of-the-art lifetimes of PEM fuel cells. Only a relatively small number of studies have investigated degradation across real PEM fuel cell lifetimes due to high costs and prolonged testing periods required. However, various ex situ accelerated tests have been proposed and implemented to explore degradation mechanisms of individual components in PEM fuel cells.

To reduce the experimental time required, different undesirable operating conditions have been utilized as the in situ accelerated stressors, such as load cycling [1,2], start–stop cycles [3], low relative humidity (RH) [4,5] or RH cycling [6], freeze–thaw cycles [7] as well as fuel [8,9] or air starvation [10]. Open circuit (OC)

operation has also been recognized as an effective stressor for accelerated testing and the accelerated effects of OC operation on the degradation of PEM fuel cell components, including the PEM and catalyst layers, have been investigated [11–15]. The increased gas crossover due to zero reactant consumption under OC conditions was believed to be the major reason for the high degradation rate of the membrane [16]. Similar to the zero electric load condition of OC operation, another effective stressor is close to OC operation, which utilizes so called idle conditions with a very low current density running on the cell. In practice, the degradation of fuel cell components under OC or idle conditions is one of the most crucial deterrents that affect a fuel cell's durability, especially for automotive fuel cell systems [17], because these two circumstances occur frequently over the entire lifetime of a PEM fuel cell. For example, the idle time may amount to several thousand hours over the entire lifetime of the fuel cell [18].

While investigating the degradation of different components, accelerated stress tests have shown that membrane degradation is one of the major failure modes of a PEM fuel cell. Various accelerated testing for membrane degradation has been conducted: for example, Fenton's test, using a H₂O₂ solution containing a trace amount of Fe²⁺, has been commonly employed as an ex situ method to analyze the chemical degradation of membranes [19,20]. The stress–strain test [21] and relative humidity (RH) cycling [6] have

* Corresponding author at: Institute for Fuel Cell Innovation, National Research Council Canada, 4250 Wesbrook Mall, Vancouver, BC, Canada V6T 1W5.
Tel.: +1 604 221 3038; fax: +1 604 221 3001.

E-mail address: haijiang.wang@nrc-cnrc.gc.ca (H. Wang).

Table 1
Properties of Nafion® PFSA membranes.

Membrane type	Typical thickness (μm)	Basis weight (gm^{-2})
NR211	25.4	50
NR212	50.8	100
N115	127	250
N117	183	360

been selected as accelerated means for understanding the mechanical degradation of membranes. Other conditions such as load cycling [22,23], and subzero storage, start-up and operation [24,25], which relate to frequent and/or severe humidity condition changes, were also addressed as accelerated stressors in membrane degradation research. Although there has been extensive research into membrane degradation, further understanding is still needed.

Previously, we looked at performance degradation of a single cell under open circuit voltage (OCV) [15] and a six-cell stack under idle conditions [26]. In this study, we will report our preliminary results of a four-cell stack degradation using Nafion membranes of different thicknesses, including N117, N115, NR212, and NR211. This four-cell stack, with a 50cm^2 active area, was tested on an Arbin 500W Fuel Cell Test Station under idle conditions. The cell performance and electrochemical characteristics were measured around every 200 h of operation. The electrochemical diagnostic tools used in this experiment included OCV, polarization curve (IV), electrochemical impedance spectroscopy (EIS), and linear sweep voltammetry (LSV). Ex situ measurements, including SEM, IR imaging, gas permeability, exhaust species detection, FTIR, and XPS, before and after degradation will be discussed in a separate paper.

2. Experimental

2.1. Fuel cell materials and testing apparatus

The fuel cell tested was a four-cell stack with an active area of 50cm^2 . The materials used were Ion Power customized catalyst coated membranes (CCMs) (N117, N115, NR212, and NR211) with a Pt catalyst loading of 0.3mg cm^{-2} supported on carbon on both sides and SGL gas diffusion layers (GDLs). The major properties of these membranes are listed in Table 1.

After assembling the MEAs in the four-cell stack, the stack was connected to the gas supplies of a 500W Arbin Test Station. In the stack the cells were named as Cell 1 (with N117 CCM), Cell 2 (with N115 CCM), Cell 3 (with NR212 CCM), and Cell 4 (with NR211 CCM) from the bottom to the top. Before activating the stack by load cycling, the stack was checked for leaking. For the activation process, each cycle consisted of a constant voltage at 1.6 V for 5 min, and a constant current at 7.5 A for 5 min. The cycle was repeated for 24 h.

After activation and before the membrane degradation test under idle conditions, the baseline performance data were measured. During the degradation test, the four-cell stack was operated at a constant current of 0.5 A (10mA cm^{-2}). The fuel cell stack temperature was kept at 70°C and air and hydrogen were fully humidified prior to their delivery into the fuel cell. The flow rates for air and hydrogen were set at 1.0 and 2.0 standard litres per minute (slpm), respectively.

2.2. In situ electrochemical measurements

Before and after every 200 h of operation under idle conditions, OCV, IV, EIS, and LSV were conducted to determine the performance, the fuel cell internal resistance, and the hydrogen crossover rate. For impedance measurements, a Solartron SI-1260 Impedance/Gain-Phase Analyzer was used in combination with

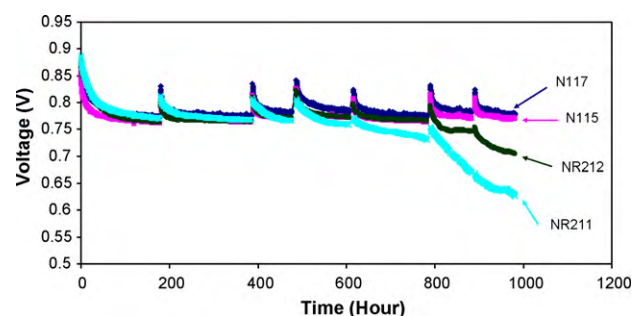


Fig. 1. Voltage degradation trends for individual cells under idle conditions for 1000 h (operating conditions: flow rate $\text{H}_2/\text{air} = 1/2$ slpm, cell temperature 70°C and fully humidified on both sides).

the Solartron SI-1287 Electrochemical Interface. For hydrogen crossover measurements, only the Solartron SI-1287 Electrochemical Interface was used.

During the polarization curve measurement, the stack was operated at 70°C and fully humidified air and hydrogen were supplied to the stack at stoichiometries of 2.5 and 1.5, respectively. When the LSV and EIS measurements were performed, the testing stack was also kept at 70°C and hydrogen and nitrogen were introduced to the anode and cathode at constant flow rates of 1.0 and 2.0 slpm, respectively. For the LSV measurement, the potential of the cathode was linearly swept from 0.05 to 0.5 V against the anode at a rate of 5mV s^{-1} . The EIS measurement was carried out at the open circuit potential. A small alternating voltage perturbation (10 mV) was imposed on the cell over a frequency range from 10 kHz to 0.03 Hz.

3. Results and discussion

3.1. Degradation curves

Fig. 1 shows the voltage degradation curves of each individual cell of the stack up to 1000 h under idle conditions (0.5A or 10mA cm^{-2}). A decreasing trend of voltage can be observed. During the 1000 h of degradation, the operation of the stack was stopped to carry out electrochemical measurements of OCV, IV, EIS, and LSV about every 200 h of operation. Two accidental shutdowns of the station occurred due to a computer update at about 500 h, and an air compressor shutdown at around 900 h. As can be seen in Fig. 1, from 600 to 800 h Cell 4, with the NR211 membrane, degrades significantly whereas other cells do not have drastic degradation; from 800 to 1000 h, both Cell 4 and Cell 3 (with the NR212 membrane) degrade dramatically while Cell 1 and Cell 2 still retain a slight degradation rate. From these results we believe that: (1) significant degradation occurred for Cell 4 during 600–800 h; (2) devastating degradation for Cell 4 and significant degradation for Cell 3 occurred during 800–1000 h. The reason for these degradations may be the membrane failure after the long-term operation, which will be examined later by other results in this work. Also, from this degradation trend we can see that for all the MEAs with membranes of different thicknesses, the voltage degradation is partially recoverable after an interruption. This is in agreement with our previous degradation tests under idle conditions [26] and OC operation [15].

The individual cell degradation rate under this accelerated stressor is listed in Table 2. At different stages, the cell degrades with a different rate. For Cell 1 and Cell 2 with thicker membranes, the degradation rate during the first 200 h was much higher than those during the subsequent periods. This phenomenon was also observed in our previous OCV experiment [15], and can be explained by the size effect of the catalyst. At the beginning of

Table 2
Degradation rate of individual cells with membranes of different thicknesses for each session.

Membrane type	0–200 h mV h ⁻¹	200–400 h mV h ⁻¹	400–600 h mV h ⁻¹	600–800 h mV h ⁻¹	800–1000 h mV h ⁻¹	Average mV h ⁻¹
N117	0.54	0.27	0.26	0.28	0.27	0.09
N115	0.53	0.21	0.21	0.25	0.22	0.09
NR212	0.65	0.20	0.19	0.19	0.45	0.18
NR211	0.64	0.21	0.25	0.25	0.64	0.26

degradation, the nano-scale catalyst particles are facile to grow at a relatively high speed under these accelerated conditions. As the degradation proceeds, the growth of the catalyst particle size becomes relatively stable. This particle size effect has also been noticed in different potential oriented experiments [27,28]. For Cell 3 and Cell 4 with thinner membranes, the degradation rate also follows the same trend as thicker membranes for about 600 h. However, when the experiment further proceeds to the last few hundred hours within this test, the degradation rates of Cell 3 and Cell 4 increase significantly, which implies the cells degrade severely. Apparently, the loss of catalyst surface area with concurrent gradual performance decrease is not the dominant failure mode in this time domain. From Table 2, we also see that the average degradation rate of each cell for the entire degradation process is much lower than those for each session, as the entire process was interrupted several times, which partially recovered the potential loss. Obviously, the degradation rates for different cells increase with decreasing the membrane thickness. In addition, the degradation rates (>0.09 mV h⁻¹) observed under idle conditions are much higher than those under steady state operation (with a degradation rate between 2 and 10 μ V h⁻¹ [29]). This can be explained by the high reactant concentration under idle conditions due to an extremely small operating current, resulting in a high reactant crossover, and then a high radical formation rate. The radicals produced are known to be the major cause for the chemical/electrochemical degradation of the membrane [30–32].

3.2. Electrochemical characterization during degradation testing

3.2.1. OCV

Fig. 2 shows the OCV degradation trend as a function of time. Similar to the degradation trend of the idle potential in Fig. 1, we can see: (1) at the very beginning and any testing times, the OCV decreases in the order of N117, N115, NR212, and NR211, due to higher hydrogen crossovers for thinner membranes (NR212 and NR211); (2) for all the MEAs with membranes of different thicknesses, the OCV degrades faster for the first 200 h; (3) after 200 h, OCVs for MEAs with thicker membranes (N117 and N115) do not change much due to unchanged hydrogen crossover; (4) dramatic OCV decay occurred for thinner membranes after 800 h of operation due to significantly increased membrane degradation. Similar phenomena were also observed for performance degradation using

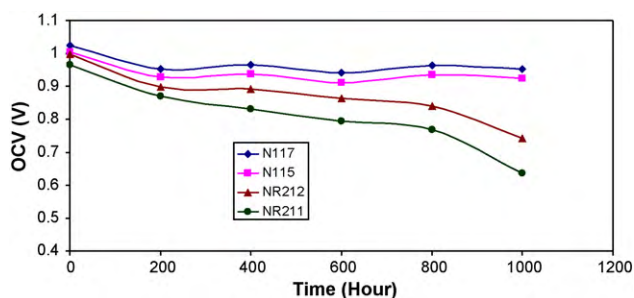


Fig. 2. OCV degradation trend for individual cells under idle conditions for 1000 h of degradation.

polarization curves. These phenomena can be attributed to the differing hydrogen crossover through membranes with different thicknesses.

Zhang et al. [33] have calculated the deviation of theoretical and measured OCVs. They believe that the OCV drop from the theoretical value is a result of the mixed potential and H₂ crossover. As expected by the prediction, they also observed that a cell with a thicker membrane would have a higher OCV due to a lower gas crossover, which completely agrees with our results shown in Fig. 2. More recently, Vilekar and Datta [34] built a model to predict the effect of H₂ permeation on OCV in PEM fuel cells. They found that hydrogen crossover is a critical parameter for OCV drop. As a result, they considered OCV as an important indicator that determines the physical well being of the membrane during prolonged operation, and identifies any membrane degradation in the form of membrane thinning or pinhole formation. In our case, we can consider that after 800 h of operation under idle conditions, membrane thinning or pinhole formation is being developed for the thinner membranes, NR212 and NR211.

3.2.2. Polarization curve

Before and after each 200 h of operation under idle conditions, polarization curves were measured to observe the performance degradation for each MEA with membranes of different thicknesses. Just as with OCV, we compared the performances of individual cells before and after each 200 h of degradation. For the thicker membranes, we can observe a marginal decrease in performance between the baseline and 200 h of degradation, and very little change after 200 h. This result agrees with what we have obtained from OCV measurements shown in Fig. 2. Similar results can also be observed for the NR212 cell and the NR211 cell within about 600 h, but another marginal decrease after 800 h.

Figs. 3 and 4, respectively, only show the performances of different cells before and after 1000 h of degradation. As we can see from these polarization curves, the current was not able to go higher than 36 A due to the high thickness of N117 membrane, limiting the proton transfer through it. It can also be seen that before degradation, the thinner the membrane is, the better the cell performs. However, after 1000 h of operation, cell performances of

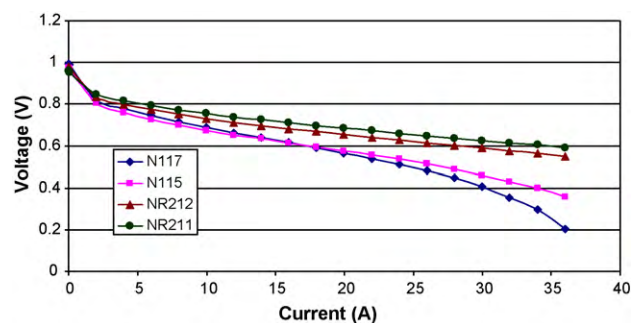


Fig. 3. Baseline polarization curves for each cell with membranes of different thicknesses before degradation (operating conditions: stoichiometry of H₂/air = 1.5/2.5 with a minimum flow rate of H₂/air = 1/2 slpm, cell temperature 70 °C and fully humidified on both sides).

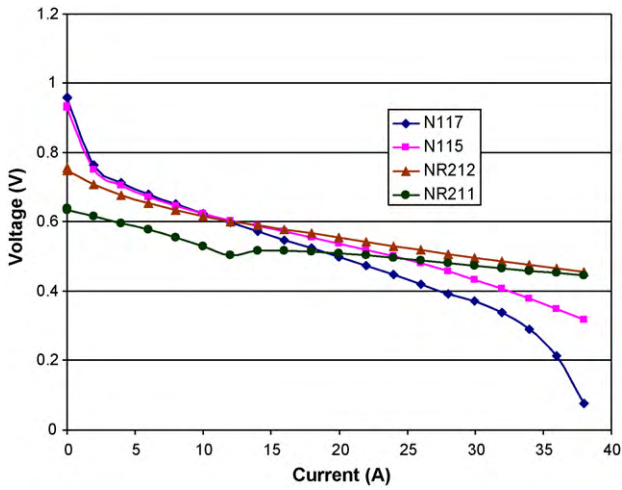


Fig. 4. Polarization curves for each cell with membranes of different thicknesses after 1000 h of degradation (operating conditions: stoichiometry of $H_2/air = 1.5/2.5$ with a minimum flow rate of $H_2/air = 1/2$ slpm, cell temperature $70^\circ C$ and fully humidified at both sides).

the thinner membranes drop significantly, indicating significant component deterioration during these 1000 h of operation. This performance deduction will be further confirmed by the LSV measurements below. Although performances for thinner membranes at low currents or current densities drop dramatically, similarly to OCV, they are still higher than thicker membranes at high currents or current densities due to the fast proton transfer through thinner membranes. Also, we noticed that after 1000 h of operation, the performance of NR211 becomes lower than that of NR212, which could be attributed to the higher hydrogen crossover through NR211.

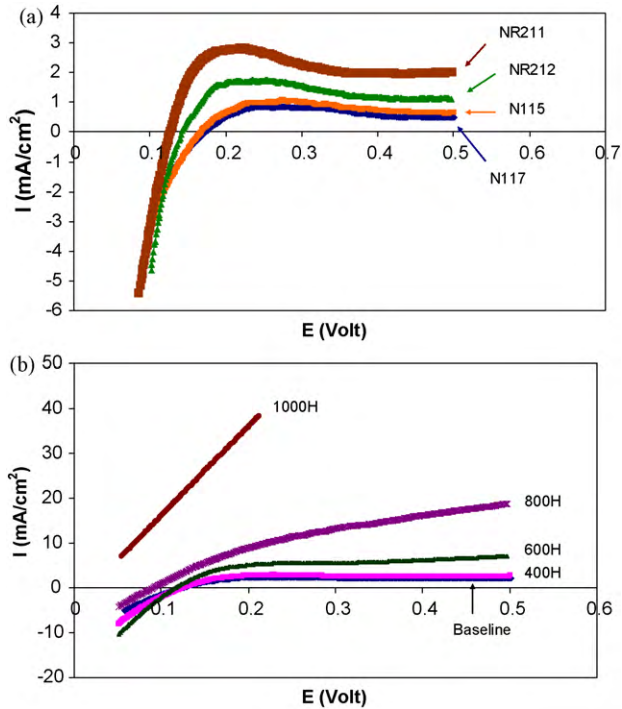


Fig. 5. (a) Comparison of hydrogen crossover through MEAs with membranes of different thicknesses before degradation and (b) comparison of hydrogen crossover through the MEA with NR211 membrane before and after degradation.

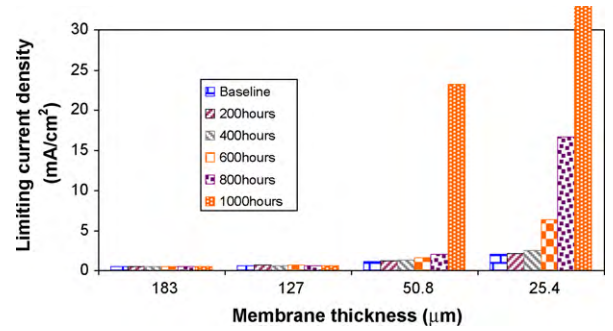


Fig. 6. The effect of thickness on hydrogen crossover through membranes at different times of degradation.

3.2.3. Hydrogen crossover

Before and after each 200 h of operation under idle conditions, a LSV was scanned to observe hydrogen crossover for each cell with different membranes. Fig. 5(a) compares the crossover limiting current of the individual cells before degradation. We can see that before degradation the thinner the membrane, the more hydrogen crosses over, which explains the lower values of OCV for cells with thinner membranes. Fig. 5(b) shows the LSV result for Cell 4 (with NR211 membrane) before and after each degradation session. An obvious crossover limiting current increase can be observed after 600 h of degradation. The hydrogen crossover is further developed significantly during the subsequent degradation session and then increases dramatically and exceeds the measurement limit of the equipment after 1000 h of degradation. This measurement confirms the dominant degradation mode switch from catalyst surface area loss to membrane decay.

The effect of thickness on hydrogen crossover with degradation for each cell is plotted in Fig. 6. It can be seen that for thicker membranes there is no significant change in hydrogen crossover before and after degradation. However, hydrogen crossover jumps significantly for NR212 after 1000 h of operation whereas for NR211 hydrogen crossover starts to increase after 600 h of operation, and keeps increasing with degradation. This result, demonstrating a faster performance degradation of thinner membranes, agrees very well with the degradation curves shown in Fig. 1, and explains the OCV degradation shown in Fig. 2, as well as performance degradation measured by polarization curves.

3.2.4. EIS

Utilizing the EIS curves before and after every 200 h of degradation, high frequency resistance (HFR) and low frequency resistance

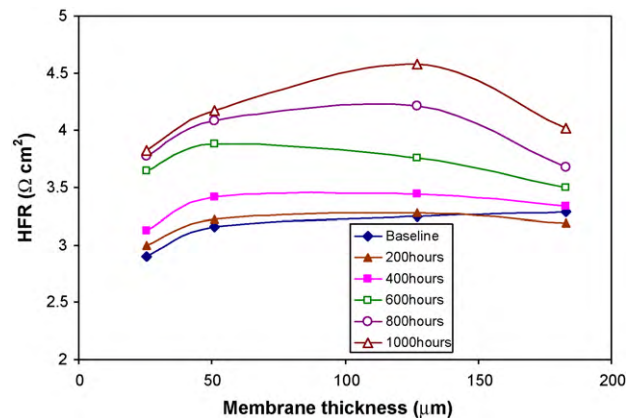


Fig. 7. Comparison of HFR for cells with membranes of different thicknesses before and after every 200 h of degradation.

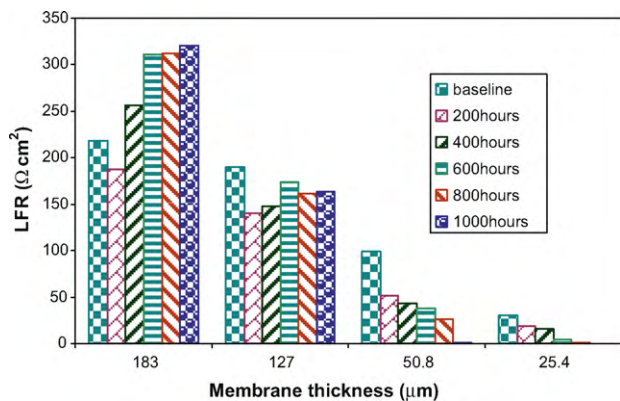


Fig. 8. Comparison of LFR for cells with membranes of different thicknesses before and after every 200 h of degradation.

(LFR) can be obtained by fitting the curves to a Randles electrical circuit. The results are plotted in Figs. 7 and 8, respectively. At the beginning of life, the HFR increases with thickness, as shown in Fig. 7. Also, for both thinner and thicker membranes, the HFR shows an obvious increasing trend with degradation, as shown in Fig. 8. This result is in good agreement with our previous results obtained under OCV and idle conditions [15,26], and could be explained by the structural and interfacial changes in the membrane due to the degradation under accelerated stressors. However, for the cell with the thickest membrane (N117), we can observe a slight decrease in HFR during the first 200 h and then an increase during the subsequent degradation sessions like the other cells. This might be attributed to the insufficient humidification of the membrane, resulting in a lower conductivity at the very beginning. Hence, at the beginning of degradation, membrane resistance is dominated by the humidity condition of the membrane. As degradation proceeds, the membranes have been fully humidified, and the structure change in the membrane becomes crucial, leading to a HFR increase with degradation time.

As for LFR, it decreases with degradation for thinner membranes, whereas for thicker membranes it decreases at the beginning of degradation, then increases. As the EIS was measured at OCV, we have:

$$\text{LFR} = \frac{RT}{nFi_0} \quad (1)$$

where R is the universal gas constant ($8.314 \text{ J mol}^{-1} \text{ K}^{-1}$), T is the temperature (K), n is the electron transfer number in the rate-determining step for oxygen reduction reaction, and F is Faraday constant ($96,485 \text{ C mol}^{-1}$). Thus, this measured LFR is related to the apparent exchange current density, i_0 (A cm^{-2}). Parameters that affect exchange current density include reaction type, catalyst, temperature, and electrolyte (membrane). Here obviously, membrane and catalyst are the two major stimuli for the measured LFR difference. As seen in Fig. 8, the thicker the membrane, the higher the LFR and the lower the apparent exchange current density resistance it has due to the higher crossover current though thinner membranes.

For thinner membranes, as the hydrogen crossover and its limiting current are much higher and increase with degradation, a steady decreasing trend of LFR can be observed. This is explained by a decrease in charge transfer resistance with current due to the increased driving force [35]. For thicker membranes, the change in hydrogen crossover before and after degradation is not obvious. Therefore, catalyst degradation plays a key role in these cases. With the progress of catalyst degradation under idle conditions, the kinetics of the ORR decreases, resulting in an increased LFR. The LFR decrease during the first 200 h of degradation might be due to the

inadequate activation of the cells with thicker membranes during the conditioning process.

4. Conclusions

Using a four-cell stack with Nafion membranes of different thicknesses, an accelerated stress test under idle conditions was carried out. The results show that the open circuit voltage (OCV) of the individual cells decreases with decreasing the membrane thickness, and it decreases much faster for thinner membranes, especially after 800 h of operation. Before degradation, the thinner the membrane, the better the cell performs. However, with the progress of degradation, the cells with thinner membranes degrade much faster with an average degradation rate of approximately 0.18 mV h^{-1} for NR212 and 0.26 mV h^{-1} for NR211, especially after 800 h, while cells with thicker membranes retain a slight degradation rate throughout the test with an average degradation rate of approximately 0.09 mV h^{-1} . The results indicate that it is the membrane degradation that accounts for the major source of the entire cell performance degradation under idle conditions. The main reason for the drastic performance decay that occurred after 800 h for thinner membranes is the dramatic increase in hydrogen crossover, while the moderate degradation for the first 800 h may result from the dominance of different degradation mechanisms, e.g., catalyst decay. Further post-analyses of the degraded MEA samples are currently being conducted to better understand the failure modes of this degradation.

Acknowledgements

The authors acknowledge the NRC-Helmholtz Joint Research program, NRC-MOST Joint Research Program, and NRC-IFCI's internal program for financial support.

References

- [1] A. Kusoglu, A.M. Karlsson, M.H. Santare, S. Cleghorn, W.B. Johnson, J. Power Sources 161 (2006) 987–996.
- [2] D. Liu, S. Case, J. Power Sources 162 (2006) 521–531.
- [3] Y. Takagia, Y. Takakuwa, ECS Trans. 3 (2006) 855–860.
- [4] J. Yu, T. Matsuura, Y. Yoshikawa, M.N. Islam, M. Hori, Phys. Chem. Chem. Phys. 7 (2005) 373–378.
- [5] E. Endoh, S. Terazono, H. Widjaja, Y. Takimoto, Electrochem. Solid-State Lett. 7 (2004) A209–A211.
- [6] X. Huang, R. Solasi, Y. Zou, M. Feshler, K. Reifsnider, D. Condit, S. Burlatsky, T. Madden, J. Polym. Sci. 16 (2006) 2346–2357.
- [7] R.C. McDonald, C.K. Mittelsteadt, E.L. Thompson, Fuel Cells 4 (2004) 208–213.
- [8] T.R. Ralph, S. Hudson, D.P. Wilkinson, ECS Trans. 1 (2006) 67–84.
- [9] A. Taniguchi, T. Akita, K. Yasuda, Y. Miyazaki, J. Power Sources 130 (2004) 42–49.
- [10] S.J.C. Cleghorn, D.K. Mayfield, D.A. Moore, J.C. Moore, G. Rusch, T.W. Sherman, N.T. Sisofo, U. Beuscher, J. Power Sources 158 (2006) 446–454.
- [11] H. Xu, R. Borup, E. Brosha, F. Garzon, B. Pivovar, ECS Trans. 6 (2007) 51–62.
- [12] T.A. Aarhaug, A.M. Svensson, ECS Trans. 3 (2006) 775–780.
- [13] S. Kundu, M. Fowler, L. Simon, R. Abouatallah, J. Power Sources 182 (2008) 254–258.
- [14] A. Ohma, S. Suga, S. Yamamoto, K. Shinohara, J. Electrochem. Soc. 154 (2007) B757–B760.
- [15] S. Zhang, X.Z. Yuan, J.N.C. Hin, H. Wang, J. Wu, K.A. Friedrich, M. Schulze, J. Power Sources 195 (2010) 1142–1148.
- [16] A. Collier, H. Wang, X. Yuan, J. Zhang, D.P. Wilkinson, Int. J. Hydrogen Energy 31 (2006) 1838–1854.
- [17] S. Sugawara, T. Maruyama, Y. Nagahara, S.S. Kocha, K. Shinohara, K. Tsujita, S. Mitsuhashi, K. Ota, J. Power Sources 187 (2009) 324–331.
- [18] M.F. Mathias, R. Makharia, H.A. Gasteiger, J.J. Conley, T.J. Fuller, G.J. Gittleman, S.S. Kocha, D.P. Miller, C.K. Mittelsteadt, T. Xie, S.G. Yan, P.T. Yu, Electrochem. Soc. Interface 14 (2005) 24–35.
- [19] A.B. LaConti, M. Hamdan, R.C. McDonald, in: W. Vielstich, H.A. Gasteiger, A. Lamm (Eds.), Handbook of Fuel Cells: Fundamentals, Technology and Applications, vol. 3, John Wiley & Sons, Ltd., 2003, pp. 647–662.
- [20] Y. Chikashige, Y. Chikyu, K. Miyatake, M. Watanabe, Macromolecules 38 (2005) 7121–7126.
- [21] P. Genova-Dimitrova, B. Baradie, D. Foscallo, C. Poinsignon, J.Y. Sanchez, J. Membr. Sci. 185 (2001) 59–71.

- [22] V.O. Mittal, H.R. Kunz, J.M. Fenton, Effect of catalyst properties on membrane degradation rate and the underlying degradation mechanism in PEMFCs, *J. Electrochem. Soc.* 153 (2006) A1755–1759.
- [23] D. Liu, S. Case, Durability study of proton exchange membrane fuel cells under dynamic testing conditions with cyclic current profile, *J. Power Sources* 162 (2006) 521–531.
- [24] Q.G. Yan, H. Toghiani, Y.-W. Lee, K.W. Liang, H. Causey, Effect of sub-freezing temperatures on a PEM fuel cell performance, startup and fuel cell components, *J. Power Sources* 160 (2006) 1242–1250.
- [25] R.C. McDonald, C.K. Mittelsteadt, E.L. Thompson, Effects of deep temperature cycling on Nafion 112 membranes and membrane electrode assemblies, *Fuel Cells* 4 (2004) 208–213.
- [26] J. Wu, X.Z. Yuan, J. Martin, H. Wang, D. Yang, J. Qiao, J. Ma, In-situ diagnosis of proton exchange membrane fuel cell degradation under close to OC condition, *J. Power Sources* 195 (2010) 1171–1176.
- [27] A.S. Aricò, A. Stassi, E. Modica, R. Ornelas, I. Gatto, E. Passalacqua, V. Antonucci, Evaluation of high temperature degradation of Pt/C Catalysts in PEM fuel cells, *ECS Trans.* 3 (2006) 765–774.
- [28] J. Xie, D.L. Wood III, K.L. More, P. Atanassov, R.L. Borup, Microstructural changes of membrane electrode assemblies during PEFC durability testing at high humidity conditions, *J. Electrochem. Soc.* 152 (2005) A1011–A1020.
- [29] J. Wu, X.Z. Yuan, J.J. Martin, H. Wang, J. Zhang, J. Shen, S. Wu, W. Merida, A review of PEM fuel cell durability: degradation mechanisms and mitigation strategies, *J. Power Sources* 108 (2008) 104–119.
- [30] F.D. Coms, The chemistry of fuel cell membrane chemical degradation, *ECS Trans.* 16 (2008) 235–255.
- [31] M.K. Kadirov, A. Bosniakovic, S. Schlick, Membrane-derived fluorinated radicals detected by electron spin resonance in UV-irradiated Nafion and Dow ionomers: effect of counterions and H₂O₂, *J. Phys. Chem. B* 109 (2005) 7664–7670.
- [32] M. Danilczuk, F.D. Coms, S. Schlick, Visualizing chemical reactions and crossover processes in a fuel cell inserted in the ESR resonator: detection by spin trapping oxygen radicals, Nafion-derived fragments, and hydrogen and deuterium adducts, *J. Phys. Chem. B* 113 (2009) 8031–8042.
- [33] J. Zhang, Y. Tang, C. Song, J. Zhang, H. Wang, PEM fuel cell open circuit voltage (OCV) in the temperature range of 23 °C to 120 °C, *J. Power Sources* 163 (2006) 532–537.
- [34] S.A. Vilekar, R. Datta, The effect of hydrogen crossover on open-circuit voltage in polymer electrolyte membrane fuel cells, *J. Power Sources* 195 (2010) 2241–2247.
- [35] X.Z. Yuan, J.C. Sun, M. Blanco, H. Wang, J. Zhang, D.P. Wilkinson, AC impedance diagnosis of a 500 W PEM fuel cell stack. Part I. Stack impedance, *J. Power Sources* 161 (2006) 920–928.